



Aerosol-cloud semi-direct effect and land-sea temperature contrast in a GCM

R. J. Allen¹ and S. C. Sherwood²

Received 5 February 2010; revised 1 March 2010; accepted 4 March 2010; published 2 April 2010.

[1] Simulations with the CAM3 climate model show that prescribed heating by anthropogenic aerosols significantly affects cloud cover. Globally the dominant effect is a decrease in mid-level clouds, which contributes to a semi-direct effect (SDE) that warms the surface by 0.5 W m^{-2} . The SDE negates some of the impact of absorbing aerosol on surface fluxes, up to 50% over the Northern Hemisphere extratropical (NHE) land during JJA. The SDE-not direct effects-drives NHE JJA warming and a land-sea contrast in surface temperature that may help explain recent trends. This behavior is mainly due to 1. the trapping of near-surface moisture associated with aerosol induced enhanced lower tropospheric stability, which preferentially increases low cloud over the sea; and 2. a burn-off of cloud, especially over land, due to reduced relative humidity in the low and middle troposphere. These effects are due to vertical redistribution of energy rather than to the horizontal heterogeneity of aerosol forcing. **Citation:** Allen, R. J., and S. C. Sherwood (2010), Aerosol-cloud semi-direct effect and land-sea temperature contrast in a GCM, *Geophys. Res. Lett.*, *37*, L07702, doi:10.1029/2010GL042759.

1. Introduction

[2] The burden of tropospheric aerosols has increased since the industrial revolution due to human activities [Bond *et al.*, 2007; Smith *et al.*, 2004]. These aerosols cool the surface directly by scattering or absorbing solar radiation, and indirectly by microphysically altering clouds [Twomey, 1977; Albrecht, 1989]. Due to their inhomogeneous spatial distribution, short lifetimes, multiple types, and complex interactions with clouds, quantifying these effects has been difficult.

[3] The absorption of sunlight by some types of aerosol like black carbon (BC) will also affect cloud cover by warming the air. Called the “semi-direct effect” (SDE) on climate, aerosol heating is expected to reduce relative humidity and thereby cloud amount and/or liquid water path, increasing surface insolation [Ackerman *et al.*, 2000; Hansen *et al.*, 1997]. This is consistent with the work of Koren *et al.* [2004], who showed that Amazonian biomass burning suppressed satellite-based cumulus cloud cover; Norris [2001], however, showed negligible changes in cloud cover over the northern Indian Ocean, despite significant increases in absorbing aerosol. The SDE has been studied

mostly in small regional cloud simulations, but since aerosol heating will drive larger-scale motions that also affect clouds, a full accounting of the effect requires a global model.

[4] There are few global estimates of the SDE due to anthropogenic aerosols. Early investigations [Lohmann and Feichter, 2001] found global SDE of about 0.1 W m^{-2} —warming about an order of magnitude smaller than the indirect cooling. Chung and Seinfeld [2005] also reported reductions in low and middle-level cloud (implying warming), but Wang [2004] found increases, leading to a negative SDE of -0.16 W m^{-2} .

[5] Much larger estimates are typically found in small-scale cloud simulations [Ackerman *et al.*, 2000; Feingold *et al.*, 2005]. For example, Johnson *et al.* [2004] find an SDE of 15 W m^{-2} for marine stratocumulus clouds due to the impact of aerosol heating on the stability of the cloud layer. One issue identified by both local [Johnson *et al.*, 2004] and global [Cook and Highwood, 2004; Yoshimori and Broccoli, 2008] studies is that the cloud response depends on the vertical aerosol heating profile, with cloudiness typically reduced at the heating level but increased below that where stability increases. Thus, uncertainties in aerosol vertical profile, optical properties [Sato *et al.*, 2003] and amounts may all contribute to the divergence of reported results.

[6] Johnson [2005] compared the behavior of the Single Column version of the Community Climate Model (SCCCM) to that of an identically forced large-eddy model, and found the SDE was five times smaller in the SCCC. This suggests that the smaller response of GCMs arises from poor cloud parameterizations rather than global dynamics, and that GCMs may be underestimating the SDE. Before accepting such a conclusion, however, more analysis of the GCM responses is warranted.

2. Experimental Design

[7] We run the standard version of the NCAR CAM3 GCM, with a slab ocean-thermodynamic sea ice model (SOM) at T42 resolution. We prescribe aerosol forcings separately in two models runs from the observationally based, global aerosol forcing data set of Chung *et al.* [2005], in two separate runs: one with anthropogenic and natural aerosols, and one with natural aerosols only (for further information, see R. J. Allen and S. C. Sherwood (The impact of natural versus anthropogenic aerosols on atmospheric circulation in the Community Atmosphere Model, submitted to *Climate Dynamics*, 2010)). Aerosol heating is uniformly distributed in the lowest 3 km of the atmosphere, in accord with observation [Ramanathan *et al.*, 2001]. The global annual mean anthropogenic aerosol forcing is 3.1 W m^{-2} in the atmosphere and -3.5 W m^{-2} at the surface (Table 1),

¹Department of Earth System Science, University of California, Irvine, California, USA.

²Climate Change Research Centre, University of New South Wales, Sydney, New South Wales, Australia.

Table 1. Summary of Global Land and Sea Annual and Jun–Jul–Aug Mean Differences for Selected Climate Variables^a

	Land		Sea	
	JJA	ANN	JJA	ANN
CBOT	0.75**	0.48**	0.37**	0.16**
CLOW	0.10	0.11	0.10*	0.06*
CMED	-0.64**	-0.48**	-0.09**	-0.11**
CHI	0.55**	0.26**	-0.08	-0.04
T_{sfc}	0.10**	0.08	0.07**	0.09**
T_{700}	0.48**	0.32**	0.17**	0.15**
S	0.44**	0.29**	0.13**	0.08**
RH ₇₀₀	-1.36**	-0.88**	-0.50**	-0.50**
RH _{BOT₃}	0.41**	0.28**	-0.02	0.05**
RH _{BOT}	0.77**	0.52**	0.14**	0.15**
Q _{BOT₃}	0.20**	0.12**	0.07**	0.06**
FSNS	-5.37**	-3.74**	-1.56**	-1.46**
FLNS	0.99**	0.66**	0.27**	0.20**
LHFLX	0.99**	0.82**	1.11**	0.95**
SHFLX	3.39**	2.26**	0.36**	0.31**
SDE _{TOA-lw}	0.08	0.04	-0.20**	-0.10**
SDE _{TOA-sw}	0.91**	0.38*	0.12	0.07
SDE _{TOA}	0.99**	0.43**	-0.08	-0.03
SDE _{SFC-lw}	-0.22**	-0.04	-0.05*	0.06**
SDE _{SFC-sw}	1.99**	1.09**	0.46**	0.29
SDE _{SFC}	1.77**	1.04**	0.41**	0.35*
F _{ATM}	7.83	5.38	2.32	1.94
F _{SFC}	-8.23	-5.75	-2.57	-2.30
F _{TOA}	-0.40	-0.37	-0.25	-0.36

^aANN, annual; JJA, Jun–Jul–Aug. Significance is denoted by bold ($\geq 90\%$); * ($\geq 95\%$) and ** ($\geq 99\%$). Also included is the prescribed aerosol direct effect at the surface (F_{SFC}) and in the atmosphere (F_{ATM}). Units for cloud (and relative humidity), temperature, specific humidity, and flux variables are %, K, g kg⁻¹ and W m⁻², respectively. Positive fluxes warm the surface. Here CBOT = cloud fraction at model's lowest level, CLOW = low-level cloud fraction, CMED = medium-level cloud fraction, CHI = high-level cloud fraction, T_{sfc} = surface temperature, T_{700} = 700 hPa temperature, S = static stability ($\theta_{700} - \theta_{sfc}$), Q_{BOT_3} = specific humidity at model's lowest 3 levels, RH_{BOT₃} = relative humidity at model's lowest 3 levels, RH_{BOT} = RH at model's lowest level, LHFLX = surface latent heat flux, SHFLX = surface sensible heat flux, FSNS = net surface shortwave radiation, FLNS = net surface longwave radiation, SDE = semi-direct effect for longwave (lw) and shortwave (sw) radiation, F_{ATM} = aerosol atmospheric heating, F_{SFC} = aerosol reduction in surface solar radiation, F_{TOA} = aerosol TOA solar forcing.

significantly greater than most previous GCM studies. We present averages from years 51–150, focusing here on the anthropogenic signal obtained from the difference of the two runs, designated ANTHRO. To explore the importance of the spatial pattern of aerosol forcing, we perform an additional experiment with horizontally uniform heating of 0.1 K day⁻¹ (about 3.5 W m⁻²) in the lowest ~3 km of the atmosphere, and compare this to an otherwise identical control run. This signal is designated as UHT.

3. Results

3.1. Cloud Response

[8] Table 1 shows global land and sea changes in low (CLOW), medium (CMED) and high (CHI) clouds for ANTHRO, along with a number of other mean quantities averaged over JJA or the whole year. High and low clouds generally increase, and mid-level clouds decrease. The increase in global and annual mean CLOW is 0.07%, of similar order to the 0.14–0.21% reported by Wang [2004] using the same model. The increase in CHI of 0.04% is qualitatively consistent with some studies [Chung and Seinfeld, 2005; Yoshimori and Broccoli, 2008; Hansen et

al., 1997; Wang, 2004]. The largest cloud signal is the -0.22% decrease in CMED.

[9] Also listed in Table 1 is the SDE (due to all clouds), which is estimated as the difference between net all-sky and clear-sky radiative fluxes for both shortwave and longwave radiation, at the TOA (top of atmosphere) and surface. For the annual global mean, the SDE is 0.11 W m⁻² at the TOA and 0.56 W m⁻² at the surface. The surface value is roughly five times larger than typical values in previous GCM studies. Both are dominated by shortwave effects, primarily due to the decrease in mid-level cloud. The SDE is much larger over land than over oceans, both at the surface (1.04 versus 0.35 W m⁻²) and TOA (0.43 versus -0.03 W m⁻²), again due mainly to larger decreases in CMED. The annual-mean changes are dominated by those in the JJA season, when the forcing is largest; changes are small south of 30S and in DJF because aerosol forcing is smaller. The rest of the paper focuses on JJA.

[10] Figure 1 (top) shows maps of the JJA changes in CLOW and CMED. There is a clear distinction between tropical (30S–30N) and NH extratropical (NHE, 30–90N) cloud changes. CLOW and CMED decrease over NHE land (-0.76% and -0.93% respectively), but increase over NHE oceans (0.60% and 0.12% (Table 2)). In the tropics, however, CLOW increases nearly everywhere (0.38%) especially over parts of Africa, while CMED decreases (-0.48% over land and -0.23% over oceans). The global means thus mask much larger systematic changes at the continental scale, including a strong land-ocean contrast in the northern extratropics. Indeed, the surface SDE is 4.29 W m⁻² over NHE land and 0.70 W m⁻² over NHE sea.

[11] These cloud changes proved robust to turning off CAM's stability-based parameterization of marine stratus (leaving in the standard RH-based scheme, which also forms low cloud). Although the tropics appear sensitive to this parameterization (CLOW over the sea increases by 0.17%, vs. -0.08% originally), changes in NHE are similar (-1.0% over land and +0.72% over sea compared to -0.76 and +0.60% originally). The SDE and NHE land-sea warming contrast are both similar.

3.2. Impact on Temperature

[12] An odd thing happens in the ANTHRO signal: the surface warms by ~0.45 K in the NHE, even though aerosols cool the surface. One might explain this as aerosol heating of the atmosphere being communicated to the surface; indeed, the 2–5 W m⁻² reduction in net solar surface heating (FSNS) is compensated by reductions in cooling by longwave, sensible and latent heat fluxes (middle section of Table 2), the largest response coming from turbulent heat fluxes (sensible on land and latent over oceans). These reductions are commensurate with, and presumably caused by, increases in lower tropospheric stability S ($\theta_{700} - \theta_{sfc}$) caused directly by the aerosol forcing.

[13] But this cannot explain the surface temperature increase, since the total aerosol forcing of the atmosphere and surface (that is, F_{TOA}) is negative (globally and in NHE). Instead the change in SFC cloud forcing (SDE_{SFC}), ~4.3 W m⁻² on land or roughly half F_{SFC} and of opposite sign, accounts for most of the warming. Thus, cloud burnoff leads to solar surface heating that well exceeds the direct cooling by the aerosols, driving land warming.

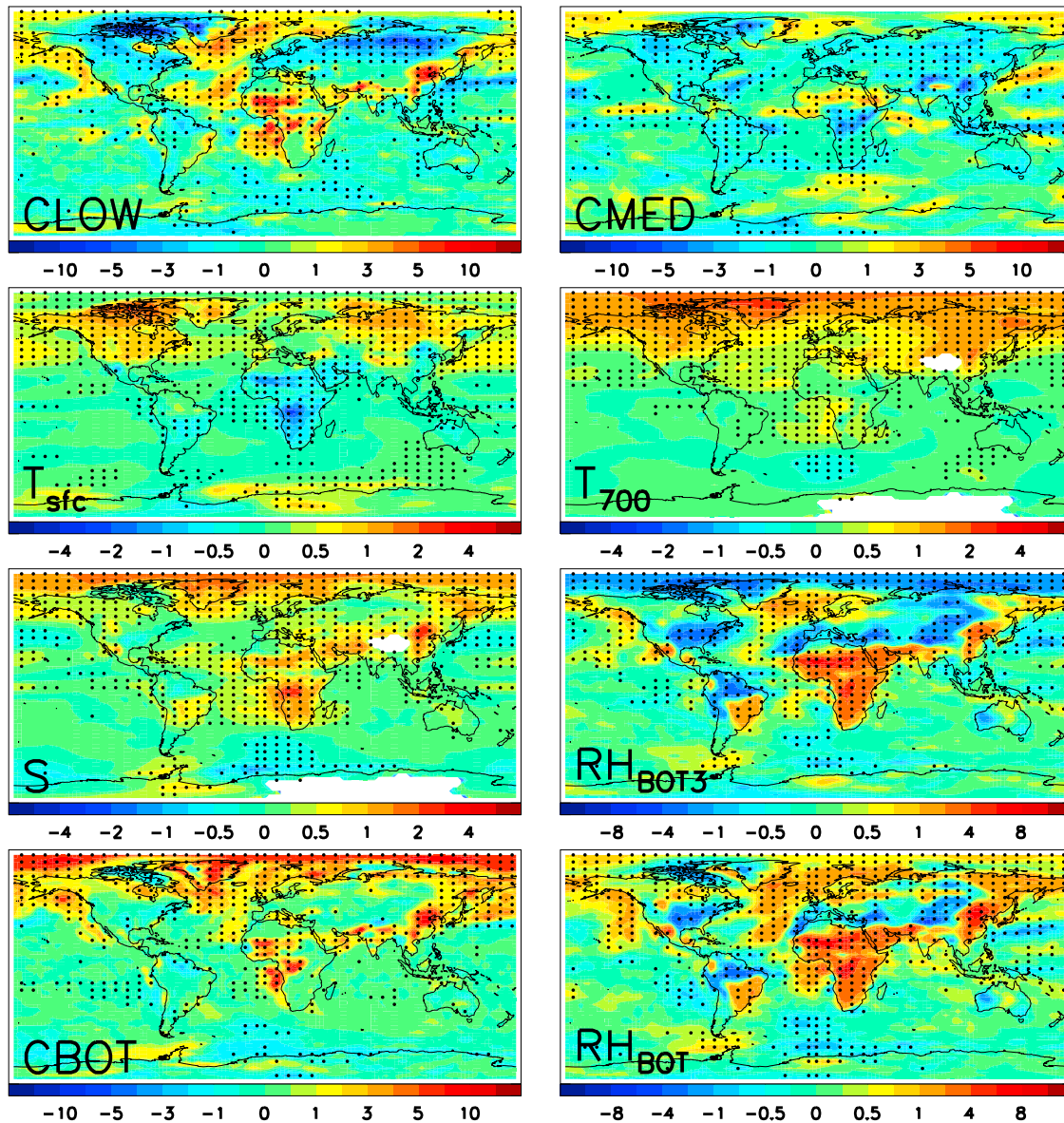


Figure 1. JJA change in (top) low and mid-level cloud; (upper middle) surface and 700 hPa temperature; (lower middle) lower-tropospheric dry static stability (S , $\theta_{700} - \theta_{sfc}$) and relative humidity for the lowest 3 model levels; and (bottom) cloud and RH for the model's bottom level. Symbols represent significance at $\geq 95\%$ confidence level. Units are % for cloud and RH variables; K for temperature variables.

3.3. Understanding the Cloud Changes

[14] We now explore the above changes in more detail by examining maps (for ANTHRO, JJA), beginning with surface and 700 hPa temperatures (Figure 1). At the surface the tropics generally cool, especially over Africa where aerosol cooling is greatest. The NH region warms significantly, especially over land. At 700 hPa, nearly the whole globe warms, especially the NH over land, contributing to the global increases in S .

[15] Figure 1 shows that similar to the CLOW/CMED changes, low-level relative humidity (lowest 3 model levels, RH_{BOT3}) decreases more over land than ocean (this is especially true in the lower troposphere, e.g., 700 hPa). Because NHE specific humidity increases similarly over land ($+0.28 \text{ g kg}^{-1}$) and ocean ($+0.31 \text{ g kg}^{-1}$), the larger

decrease in RH_{BOT3} over land is due to the larger warming. Figure 1 also shows that RH at the bottom model level (RH_{BOT}) increases, by twice as much over oceans (0.51%) as land (0.26%). This difference is associated with a larger increase in CBOT (1.78% versus 0.96%), suggesting that aerosol heating traps humidity near the surface, especially over ocean, increasing low cloud. A possible issue, however, is that CAM tends to produce too much low cloud in general [Collins *et al.*, 2006].

[16] We quantified the roles of three predictors of simulated cloud- S [Klein and Hartmann, 1993], RH [Bretherton *et al.*, 1995] and vertical motion [Norris and Klein, 2000]—using regression models applied to data from the control simulation (the experiment run yields similar results). Because of differing cloud behavior we fit models independently to land and ocean data for the tropics, NHE, and SHE

Table 2. As in Table 1, but for the Northern Hemisphere Extratropics During JJA for Both ANTHRO and UHT^a

	ANTHRO		UHT	
	Land	Sea	Land	Sea
CBOT	0.96**	1.78**	0.00	0.74**
CLOW	-0.76**	0.60**	-1.21**	-0.55**
CMED	-0.93**	0.12	-0.73**	0.15
CHI	0.44**	0.39**	0.96**	1.04**
T_{sfc}	0.56**	0.39**	1.04**	0.91**
T_{700}	0.93**	0.65**	1.02**	0.92**
S	0.44**	0.32**	0.09	0.11
RH ₇₀₀	-1.74**	-0.11	-1.08**	-0.82**
RH _{BOT₃}	-0.40**	-0.21**	-0.46	-0.18
RH _{BOT}	0.26	0.51**	-0.13	0.18*
Q _{BOT₃}	0.28**	0.31**	0.40**	0.50**
FSNS	-4.50**	-2.24**	2.88**	1.88**
FLNS	0.18	1.52**	-0.47	0.43*
LHFLX	1.06**	1.88**	-2.99**	-0.81*
SHFLX	3.46**	0.56**	0.39	0.35**
SDE _{TOA_{lw}}	-0.33**	-0.16	0.46**	0.71**
SDE _{TOA_{sw}}	2.87**	-0.40	2.17**	0.25
SDE _{TOA}	2.54**	-0.56*	2.62**	0.96**
SDE _{SFC_{lw}}	-0.92**	-0.33**	-1.29**	-1.01**
SDE _{SFC_{sw}}	5.21**	1.03**	2.76**	0.78
SDE _{SFC}	4.29**	0.70*	1.48**	-0.23
F _{ATM}	8.47	3.52	~3.5	~3.5
F _{SFC}	-9.19	-3.78	0	0
F _{TOA}	-0.73	-0.28	~3.5	~3.5

^aNorthern Hemisphere extratropics, 30–90°N. Significance is denoted by bold ($\geq 90\%$); * ($\geq 95\%$) and ** ($\geq 99\%$).

region. We find that the best model uses both S and RH (at the lowest three model levels for CLOW and 600 hPa for CMED). In the NHE, the model R^2 ranges from 0.72 (for CLOW over oceans) to 0.89 (for CMED over land). In the tropics, the model R^2 ranges from 0.57 (for CLOW over land) to 0.81 (for CMED over land). RH is the stronger predictor in the extratropics, and S the stronger in the tropics; the signs of all regression coefficients are positive as expected.

[17] The bivariate regression models predict fairly well the changes in mean CLOW and CMED in ANTHRO given the changes in mean RH_{BOT₃} and S . The predicted (actual) changes over NHE land are -0.81% (-0.76%) for CLOW and -0.51% (-0.93%) for CMED; those over NHE oceans are 0.49% (0.60%) for CLOW and 0.08% (0.12%) for CMED. Similar skill levels are shown for the tropical changes. These predictions are generally superior to those from regression models based on S or RH_{BOT₃} alone, and show that the semi-direct effects can mostly be explained by aerosol-driven changes to stability and humidity.

[18] A similar analysis was performed to predict near-surface RH (RH_{BOT}) from S , which is strongly correlated in the simulated climate (R^2 ranging from 0.18 over tropical oceans to 0.60 over NHE land). The predicted changes in mean RH_{BOT} were accurate, especially over oceans: $+0.52\%$ predicted vs. 0.51% actual for NHE, and 0.15% vs. 0.13% in the tropics. This supports the notion that the stabilizing effect of aerosol heating traps humidity near the surface.

[19] The broad-scale changes reported above are similar in our UHT experiment. Table 2 shows similar cloud changes (although CLOW decreases over the sea), which leads to a corresponding, although somewhat weaker, land-sea warming contrast. A similar trapping of near-surface marine humidity also occurs, consistent with a larger increase in CBOT ($+0.74\%$ versus $+0.0\%$ over land). This experiment suggests the RH_{BOT} contrast is due to a larger increase in

Q_{BOT} over the ocean (25 percent increase), implying that moisture limitations inhibit the increase over land. Nonetheless, even if the near-surface humidity increase were uniform, we would still expect a larger increase in cloud over the ocean because marine air is generally closer to saturation. Thus the impacts, including the land-ocean contrast of cloud and other changes, are due mainly to the vertical redistribution of energy by the aerosols rather than the horizontally heterogeneous nature of the forcing.

4. Discussion

[20] The land-sea warming contrast exhibited here also occurs in climate model simulations forced with increased greenhouse gases [e.g., *Manabe et al.*, 1991], but not as strongly as recently observed in the NHE [*Sutton et al.*, 2007]. Most studies attribute this contrast to more efficient cooling of oceans by evaporation, although recent studies show the importance of lapse rates and large-scale cloud [*Joshi et al.*, 2007], as well as the physiological effect of CO₂ on plant stomatal conductance [*Doutriaux-Boucher et al.*, 2009]. Our results suggest that aerosol-induced cloud effects may also contribute to the observed land-sea warming trend contrast. This effect would have been underrepresented in the IPCC AR4 models, for example, due to underestimation of aerosol absorption [*Sato et al.*, 2003].

[21] We propose the following hypothesis to explain the cloud changes and corresponding semi-direct effects in our simulations. Heating the lowest ~ 3 km tends globally to reduce RH above the ABL and throughout the lower troposphere—especially over land where moisture is limited—and increase lower tropospheric static stability. The first would tend to inhibit low cloud, the latter enhance it. An increase in S also inhibits vertical mixing, trapping moisture near the surface, especially over the oceans where there are no moisture limitations. This promotes increases in low cloud. Over tropical oceans, dominant cloud types are marine stratocumulus and trade cumulus [e.g., *Rossow and Schiffer*, 1991]. These should increase due to S [e.g., *Klein and Hartmann*, 1993] but may be too shallow to be affected by relative humidity reductions above the ABL. Midlatitude low and mid-level clouds however are largely associated with deeper synoptic flows and would be more tightly connected to RH. Above the ABL, a burn-off by the widespread reductions in RH due to warming over land would, therefore, explain the midlatitude cloud decreases over land; over the sea, however, increased near-surface RH (i.e., RH_{BOT}) explains the increase in CLOW. Over warmer tropical surfaces the RH and S changes should inhibit mid-level cloud but enhance the deep convection, explaining the reduced CMED.

5. Conclusions

[22] We find a significant positive semi-direct effect, due to reductions of primarily mid-level but also low cloud, up to five times larger at the surface (0.56 W m^{-2}) than previously reported, though no larger at top of atmosphere than found elsewhere ($\sim 0.1 \text{ W m}^{-2}$). A new finding is that semi-direct cloud changes are very different on land and ocean, driving land-sea warming contrasts, especially in northern midlatitudes during summer. This warming contrast is due not only to less evaporative cooling over land, as shown by

Manabe *et al.* [1991] and Sutton *et al.* [2007], but also because of increased solar heating due to decreased low and mid-level clouds caused by aerosol heating of the lower troposphere. Trends in aerosol forcing could thereby help explain the land-sea NHE trend [Sutton *et al.*, 2007].

[23] The robustness of this result to model used remains to be demonstrated, though we have shown that the key result remains similar with removal of CAM's stability-based low cloud parameterization. We conclude that anthropogenic aerosol heating may have larger effects on cloud cover and surface energy budgets than previously estimated, appears to drive land-sea contrasts, and should be more carefully considered in future studies.

[24] **Acknowledgments.** This study was funded by the NSF (CA-REER ATM-0453639), Yale University, and by NSF ARC-0714088 and NASA NNX07AR23G, UC Irvine. We thank Chul Eddy Chung, Charlie Zender, Dorothy Koch and an anonymous reviewer for their comments and suggestions.

References

- Ackerman, A. S., O. B. Toon, D. E. Stevens, A. J. Heymsfield, V. Ramanathan, and E. J. Welton (2000), Reduction of tropical cloudiness by soot, *Science*, *288*, 1042–1047.
- Albrecht, B. A. (1989), Aerosols, cloud microphysics, and fractional cloudiness, *Science*, *245*, 1227–1230.
- Bond, T. C., E. Bhardwaj, R. Dong, R. Jogani, S. Jung, C. Roden, D. G. Streets, and N. M. Trautmann (2007), Historical emissions of black and organic carbon aerosol from energy-related combustion, 1850–2000, *Global Biogeochem. Cycles*, *21*, GB2018, doi:10.1029/2006GB002840.
- Bretherton, C. S., E. Klinker, A. K. Betts, and J. A. Coakley (1995), Comparison of ceilometer, satellite, and synoptic measurements of boundary-layer cloudiness and the ECMWF diagnostic cloud parameterization scheme during ASTEX, *J. Atmos. Sci.*, *52*, 2736–2751.
- Chung, C. E., V. Ramanathan, D. Kim, and I. A. Podgorny (2005), Global anthropogenic aerosol direct forcing derived from satellite and ground-based observations, *J. Geophys. Res.*, *110*, D24207, doi:10.1029/2005JD006356.
- Chung, S. H., and J. H. Seinfeld (2005), Climate response of direct radiative forcing of anthropogenic black carbon, *J. Geophys. Res.*, *110*, D11102, doi:10.1029/2004JD005441.
- Collins, W. D., P. J. Rasch, B. A. Boville, J. J. Hack, J. R. McCaa, D. L. Williamson, and B. P. Briegleb (2006), The formulation and atmospheric simulation of the Community Atmosphere Model: CAM3, *J. Clim.*, *19*, 2144–2161.
- Cook, J., and J. Highwood (2004), Climate response to tropospheric absorbing aerosols in an intermediate general-circulation model, *Q. J. R. Meteorol. Soc.*, *130*, 175–191.
- Doutriaux-Boucher, M., M. J. Webb, J. M. Gregory, and O. Boucher (2009), Carbon dioxide induced stomatal closure increases radiative forcing via a rapid reduction in low cloud, *Geophys. Res. Lett.*, *36*, L02703, doi:10.1029/2008GL036273.
- Feingold, G., H. Jiang, and J. Y. Harrington (2005), On smoke suppression of clouds in Amazonia, *Geophys. Res. Lett.*, *32*, L02804, doi:10.1029/2004GL021369.
- Hansen, J., M. Sato, and R. Ruedy (1997), Radiative forcing and climate response, *J. Geophys. Res.*, *102*, 6831–6864.
- Johnson, B. T. (2005), The semidirect aerosol effect: Comparison of a single-column model with large eddy simulation for marine stratocumulus, *J. Clim.*, *18*, 119–130.
- Johnson, B. T., K. P. Shine, and P. M. Forster (2004), The semi-direct aerosol effect: Impact of absorbing aerosols on marine stratocumulus, *Q. J. R. Meteorol. Soc.*, *130*, 1407–1422.
- Joshi, M. M., J. M. Gregory, M. J. Webb, D. M. H. Sexton, and T. C. Johns (2007), Mechanisms for the land/sea warming contrast exhibited by simulations of climate change, *Clim. Dyn.*, *30*, 455–465, doi:10.1007/s00382-007-0306-1.
- Klein, S. A., and D. L. Hartmann (1993), The seasonal cycle of low stratiform clouds, *J. Clim.*, *6*, 1587–1606.
- Koren, I., Y. J. Kaufman, L. A. Remer, and J. V. Martins (2004), Measurement of the effect of Amazon smoke on inhibition of cloud formation, *Science*, *303*, 1342–1345.
- Lohmann, U., and J. Feichter (2001), Can the direct and semi-direct aerosol effect compete with the indirect effect on a global scale?, *Geophys. Res. Lett.*, *28*, 159–161.
- Manabe, S., R. J. Stouffer, M. J. Spelman, and K. Bryan (1991), Transient responses of a coupled ocean-atmosphere model to gradual changes of atmospheric CO₂. Part I: Annual mean response, *J. Clim.*, *4*, 785–818.
- Norris, J. R. (2001), Has northern Indian Ocean cloud cover changed due to increasing anthropogenic aerosol?, *Geophys. Res. Lett.*, *28*, 3271–3274.
- Norris, J. R., and S. A. Klein (2000), Low cloud type over the ocean from surface observations. Part III: Relationship to vertical motion and the regional surface synoptic environment, *J. Clim.*, *13*, 245–256.
- Ramanathan, V., et al. (2001), Indian Ocean Experiment: An integrated analysis of the climate forcing and effects of the great Indo-Asian haze, *J. Geophys. Res.*, *106*, 28,371–28,398.
- Rossow, W. B., and R. A. Schiffer (1991), ISCCP cloud data products, *Bull. Am. Meteorol. Soc.*, *72*, 2–20.
- Sato, M., J. Hansen, D. Koch, A. Lacis, R. Ruedy, O. Dubovik, B. Holben, M. Chin, and T. Novakov (2003), Global atmospheric black carbon inferred from AERONET, *Proc. Natl. Acad. Sci. U. S. A.*, *100*, 6319–6324.
- Smith, S., R. Andres, E. Conception, and J. Lurz (2004), Historical sulfur dioxide emissions 1850–2000: Methods and results, *Tech. Rep. PNNL-14537*, Joint Global Change Res. Inst., College Park, Md.
- Sutton, R. T., B. Dong, and J. M. Gregory (2007), Land/sea warming ratio in response to climate change: IPCC AR4 model results and comparison with observations, *Geophys. Res. Lett.*, *34*, L02701, doi:10.1029/2006GL028164.
- Twomey, S. (1977), The influence of pollution on the shortwave albedo of clouds, *J. Atmos. Sci.*, *34*, 1149–1152.
- Wang, C. (2004), A modeling study on the climate impacts of black carbon aerosols, *J. Geophys. Res.*, *109*, D03106, doi:10.1029/2003JD004084.
- Yoshimori, M., and A. J. Broccoli (2008), Equilibrium response of an atmosphere-mixed layer ocean model to different radiative forcing agents: Global and zonal mean response, *J. Clim.*, *21*, 4399–4423.

R. J. Allen, Department of Earth System Science, University of California, Irvine, CA 92697, USA. (rjallen@uci.edu)
S. C. Sherwood, Climate Change Research Centre, University of New South Wales, Sydney, New South Wales 2052, Australia.